Global Change Biology (2009) **15**, 961–975, doi: 10.1111/j.1365-2486.2008.01735.x

Leaf phenology in 22 North American tree species during the 21st century

XAVIER MORIN*†, MARTIN J. LECHOWICZ†, CAROL AUGSPURGER‡, JOHN O'KEEFE§, DAVID VINER¶ and ISABELLE CHUINE*

Centre d'Ecologie Fonctionnelle et Evolutive, Equipe Bioflux, CNRS, 1919 route de Mende, 34293 Montpellier Cedex 5, France, †Biology Department, McGill University, 1205 Dr Penfield Avenue, Montreal, QC, Canada H3A 1B1, ‡Department of Plant Biology, University of Illinois, 505 S. Goodwin Avenue, Urbana, IL 61801, USA, §Harvard University, Harvard Forest, Petersham, MA 01366, USA, ¶Natural England, Science and Evidence, 60 Bracondale, Norwich NR1 2BE, UK

Abstract

Recent shifts in phenology are the best documented biological response to current anthropogenic climate change, yet remain poorly understood from a functional point of view. Prevailing analyses are phenomenological and approximate, only correlating temperature records to imprecise records of phenological events. To advance our understanding of phenological responses to climate change, we developed, calibrated, and validated process-based models of leaf unfolding for 22 North American tree species. Using daily meteorological data predicted by two scenarios (A2: + 3.2 °C and B2: + 1 °C) from the HadCM3 GCM, we predicted and compared range-wide shifts of leaf unfolding in the 20th and 21st centuries for each species. Model predictions suggest that climate change will affect leaf phenology in almost all species studied, with an average advancement during the 21st century of 5.0 days in the A2 scenario and 9.2 days in the B2 scenario. Our model also suggests that lack of sufficient chilling temperatures to break bud dormancy will decrease the rate of advancement in leaf unfolding date during the 21st century for many species. Some temperate species may even have years with abnormal budburst due to insufficient chilling. Species fell into two groups based on their sensitivity to climate change: (1) species that consistently had a greater advance in their leaf unfolding date with increasing latitude and (2) species in which the advance in leaf unfolding differed from the center to the northern vs. southern margins of their range. At the interspecific level, we predicted that early-leafing species tended to show a greater advance in leaf unfolding date than late-leafing species; and that species with larger ranges tend to show stronger phenological changes. These predicted changes in phenology have significant implications for the frost susceptibility of species, their interspecific relationships, and their distributional shifts.

Keywords: climate change, comparative analysis, geographical distribution, leaf phenology, North America, process-based modeling, trees

Received 9 January 2008; revised version received 17 June 2008 and accepted 28 August 2008

Introduction

Impacts of current climate change have been observed in a variety of ecosystems and biological processes (Parmesan, 2006). Because phenological events are strongly responsive to temperature, they have been among the first documented fingerprints of climate change (Menzel & Fabian, 1999; Menzel *et al*., 2006), and reported examples are more numerous every year (Beaubien & Freeland, 2000; Abu-Asab *et al*., 2001; Walther *et al*., 2001; Ahas *et al*., 2002; Penuelas & Boada, 2003; Root *et al*., 2003; Defila & Clot, 2005; Wolfe *et al*., 2005; Menzel *et al*., 2006). The growing season of trees has been extended on average by 2.3 days decade^{-1} during the last 40 years (Myneni *et al*., 1997; Parmesan

Correspondence: Xavier Morin, Biology Department, McGill University, 1205 Dr Penfield Avenue, Montreal, QC, Canada H3A 1B1, tel. + 1 514 398 4116, fax + 1 514 398 5069, e-mail: xavier.morin@mail.mcgill.ca

& Yohe, 2003). Focusing on a few selected temperate tree species, Richardson *et al*. (2006) found similar rates (e.g. 2.1 days longer decade^{-1} for *Acer saccharum*). This trend is predicted to continue according to climate conditions forecast for the next century (IPCC, 2007). Increasing phenological changes in temperate forests are likely to have strong impacts on both tree species' distribution (Chuine & Beaubien, 2001) and productivity (Loustau *et al*., 2005). Phenological changes can affect the cold hardiness of species (Cannell, 1985; Hänninen, 1991), increasing frost injury and winter hardening and thereby affecting survival and growth. As forests play a major role in the terrestrial storage of carbon, any changes in their distribution will have important implications, not only for forest products and biodiversity, but also for the global climate itself (Sitch *et al*., 2003). Accurate predictions of tree phenology therefore are necessary to understand the impact of climate change on forest ecosystems.

Both experimental and modeling studies have been used to predict tree phenology. Provenance transfer experiments have been carried out to simulate changes in temperature (e.g. Hänninen, 1996). However, these experiments impose an abrupt temperature change to individuals that are moved far away from their latitude of origin, and simulate a greater increase in temperature than climate change predictions.

Focusing on modeling, three categories of phenological models can be identified: theoretical, statistical, and process-based models. Theoretical models (Kikuzawa, 1991, 1995) have been developed to understand the cost and benefits related to the timing of production of leaves, but these models cannot be used to predict the timing of budburst at the species level. Statistical models (Boyer, 1973; Spieksma *et al*., 1995; Schwartz, 1998) use linear equations to relate atmospheric conditions and leaf unfolding dates. These models can thus provide information about general trends of phenological changes under global warming, but their biological interpretation is necessarily limited. Process-based models, which trace back to the pioneering work of Sarvas (1972, 1974), have improved steadily, especially in the last decade. The simplistic spring warming models, relying on the accumulation of growing degree days (Cannell & Smith, 1983; Hunter & Lechowicz, 1992) have evolved into more mechanistic models of tree phenology (Kramer, 1994; Chuine & Cour, 1999; Chuine, 2000) that are increasingly sophisticated (Linkosalo, 2000; Linkosalo *et al*., 2006). Chuine *et al*. (2003) and Hänninen & Kramer (2007) provide recent, thorough reviews of these process-based models.

In this study, we first build on the legacy of past work to develop, calibrate, and validate process-based phenological models for leaf unfolding in each of 18 Eastern North American tree species. Second, using the climate predictions of the GCM HadCM3 for the IPCC storylines A2 and B2, we simulated the yearly change in the leaf unfolding date in the 20th into the 21st century for these 18 species and four others previously calibrated. Third, we identified and compared groups of phenological responses to climate change among these 22 species based on trends in leaf unfolding date predicted for the 21st century. Our overall objectives were: (1) to make an initial assessment of alternative phenological responses to climate change among North American trees and (2) to identify fruitful avenues for experimental and observational studies that would contribute to improving the predictions of process-based phenological models.

Materials and methods

We developed models predicting the date of leaf unfolding (date of first fully formed leaf) for 18 North American temperate tree species representing 11 genera (Table 1). Using these models, as well as previously developed models for four other species (Chuine *et al*., 2001, 2006; Chuine & Beaubien, 2001), we simulated leaf unfolding date for 22 species representing 13 genera for every year in the 20th and 21st centuries (Table 2).

Datasets

Times series of leaf unfolding dates were available for natural populations in three locations (Table 1): Wauseon, OH (41°33′N, −84°09′W; Smith, 1915), Harvard Forest, MA (42°53′N; 72°19′W; unpublished data, http://harvardforest.fas.harvard.edu/data/p00/hf003/HF003-data.html), and Urbana, IL (40°N, 88°W; C. Augspurger, unpublished data). The Wauseon data were recorded between 1883 and 1912, the Harvard and Urbana data between 1990 and 2003. Daily meteorological data were available for all three locations. The current distributions of species were taken from USDA Forest Service maps compiled by Critchfield and Little (Critchfield & Little, 1966; Little, 1971, 1976, 1977; http://climchange.cr.usgs.gov/data/atlas/little).

Phenological models

Leaf unfolding was modeled in the framework of a Unified General Model (Chuine, 2000) that is defined by nine specific parameters, but that can be simplified when appropriate by using simpler parameterization for chilling and/or forcing processes as in Richardson *et al*. (2006). Our simplified models are described in Appendix S1.

The leaf unfolding date (D_l) was simulated following the full Unified model developed by Chuine

Table 1 Parameter estimates, goodness of fit, and external validation of the leaf unfolding date models for 18 species

Species	*p*	*n*	*m*	*a*	*b*	*c*	*d*	*e*	*w*	*z*	C_c	t_c	t_1	F_c	Name	Location	RMSE	r^2	r^2 cross	ΔAIC_c
Acer saccharinum	1	26	9	0.80	−29.99	8.75	−0.58	−12.05	2138.40	−0.05	89.83	103.89	–	–	OH	41°33′; −84°09′	3.40	0.77	0.55	
Acer rubrum	1	13	9	0.54	−17.36	−24.59	−22.03	8.48	598.72	−0.02	64.88	292.65	–	–24.59	MA	42°53′; −72°09′	1.93	0.88	–	
Aesculus glabra	1	11	3	–	–	–	–	9.43	–	–	–	–	190.89	26.64	IL	40°; −88°	3.62	0.49	–	−50.1
Carya glabra	1	19	7	–	–	12.71	−2.40	−12.48	676.70	−0.02	179.83	288.81	–	–	OH	41°33′; −84°09′	1.81	0.94	0.80	−19.5
Carya ovata	2	21	9	1.04	−28.74	10.01	−0.94	−13.09	64.46	−0.01	85.15	122.11	–	–	OH	41°33′; −84°09′	1.96	0.93	0.66	
		11	3	–	–	–	–	−11.93	–	–	–	–	143.72	102.73	IL	40°; −88°	3.41	0.23	–	−71.3
Fraxinus nigra	1	16	9	0.42	15.00	−12.68	−1.57	−12.12	350.56	−0.01	179.66	268.43	–	–	OH	41°33′; −84°09′	1.93	0.94	0.73	
Fraxinus americana	3	19	9	0.65	−25.26	26.59	−0.62	−11.43	1523.62	−0.02	147.67	228.77	–	–	OH	41°33′; −84°09′	2.63	0.89	0.59	
		13	7	–	–	18.96	−0.29	−19.98	2115.58	−0.03	157.67	255.76	–	–	MA	42°53′; −72°09′	−1.55	0.87	–	−9.1
		11	4	–	–	–	−0.24	−18.27	–	–	–	–	215.56	15.82	IL	40°; −88°	1.70	0.87	–	−7.6
Juglans nigra	2	19	3	–	–	–	–	6.35	–	–	–	–	217.63	33.00	OH	41°33′; −84°09′	2.94	0.81	0.80	−7.0
		11	9	0.57	−15.34	6.10	−16.18	−18.95	962.88	−0.02	155.95	252.89	–	–	IL	40°; −88°	1.23	0.94	–	
Ostrya virginiana	1	18	7	–	–	28.25	−40.00	−9.86	829.88	−0.02	230.23	243.84	–	–	OH	41°33′; −84°09′	3.62	0.62	0.43	−8.2
Platanus occidentalis	1	19	3	–	–	–	–	6.36	–	–	–	–	220.65	33.58	OH	41°33′; −84°09′	3.95	0.62	0.69	−25.8
Quercus alba	1	13	7	–	–	14.84	−0.49	−15.73	1299.39	−0.02	125.48	257.75	–	–	MA	42°53′; −72°09′	2.80	0.79	–	−3.6
Quercus bicolor	1	17	9	0.41	15.00	−12.57	−0.45	−15.18	418.00	−0.02	90.99	249.08	–	–	OH	41°33′; −84°09′	2.09	0.93	0.64	
Quercus macrocarpa	1	19	3	–	–	–	–	9.93	–	–	–	–	228.51	18.62	OH	41°33′; −84°09′	2.32	0.88	0.74	−15.5
Quercus rubra	1	13	7	–	–	8.41	−22.51	−12.55	2705.09	−0.03	39.96	266.82	–	–	MA	42°53′; −72°09′	2.57	0.78	–	−6.1
Quercus velutina	1	19	3	–	–	–	–	9.71	–	–	–	–	227.62	19.10	OH	41°33′; −84°09′	2.49	0.88	0.76	−7.3
Salix nigra	1	21	4	–	–	–	−0.40	−19.91	–	–	–	–	78.47	2.01	OH	41°33′; −84°09′	4.27	0.59	0.50	−3.3
Sassafras albidum	1	21	4	–	–	–	−0.43	−12.12	–	–	–	–	63.25	23.31	OH	41°33′; −84°09′	2.86	0.85	0.53	−2.7
Ulmus americana	2	26	9	0.59	−18.56	15.38	−0.55	−12.44	548.50	−0.02	185.00	266.00	–	–	OH	41°33′; −84°09′	3.04	0.72	0.49	
		11	8	3.15	−10.62	−6.09	0.00	9.59	92.25	−0.05	1.08	78.67	–	–	IL	40°; −88°	3.17	0.66	–	−24.8

p, number of populations available for each species; *n*, number of observations per population; *m*, number of parameters of the selected model. *a*, *b*, *c*, *d*, *e*, *w*, *z*, C_c, t_c (specific parameters for the Unified model, and for seven- and eight-parameters models), t_1, F_c (specific parameters for the three- and four-parameters models): parameter estimates of each model (see 'Materials and methods', Appendix S1, and Chuine, 2000). *Name*: name of the population; OH: Wauseon, Ohio; MA: Harvard, Massachussets; IL: Urbana, Illinois. RMSE: root mean square error of the predictions in comparison with data. r^2: efficiency of the model in the calibration dataset (r^2 coefficients are provided but should be interpreted with caution, as there is no well-defined equivalent for nonlinear models); r^2 cross: efficiency of the model in the validation dataset; ΔAIC_c: difference of AIC_c between the simplified model chosen and the Unified model (with nine parameters).

Table 2 Mean simulated date of leaf unfolding (in day of the year) over the 20th century (L); mean number of days of change in the date of leaf unfolding simulated for the 21st century in comparison with L for scenarios A2 and B2 (L_{A2} and L_{B2}, respectively) (positive values indicate a later date; negative values an earlier date); mean number of years with abnormal leaf unfolding occurrence in the 21st century (P_{A2} and P_{B2} for each scenario); total (C_{A2}, C_{B2}) and relative (S_{A2}, S_{B2}) change in leafing date in both scenarios (for S_{A2} and S_{B2}, positive values indicate that most pixels in the distribution exhibit a delay in the leaf unfolding date; negative values indicate that most pixels in the distribution exhibit an earlier leaf unfolding date); group of response to which the species belongs: A (latitudinal response), B (centrifugal response) (*Group*) (see text for explanations); number of pixels ($0.5^\circ \times 0.5^\circ$) occupied by each species' distribution (*Range*)

Species	L	L_{A2}	L_{B2}	P_{A2}	P_{B2}	C_{A2}	C_{B2}	S_{A2}	S_{B2}	Group	Range
Acer rubrum	134	−1.0	−0.6	3.7	6.2	0.68	0.76	0.16	0.14	A	1372
Acer saccharinum	100	−5.8	−20.1	11.2	4.8	0.92	0.91	0.22	−0.38	A	1059
Acer saccharum	123	−2.6	−3.2	1.9	3.9	0.57	0.77	−0.35	−0.39	A	1013
Aesculus glabra	117	−4.0	−6.9	0	0	0.63	0.94	−0.63	−0.94	A	387
Carya glabra	146	0.3	−14.8	27.9	29.1	0.49	0.48	0.43	0.45	B	787
Carya ovata	128	2.7	−15.7	12.6	7.8	0.59	0.99	0.02	−0.99	A	859
Fraxinus americana	138	−12.4	−17.2	−0.7	−0.4	0.74	0.79	−0.45	−0.65	A	1214
Fraxinus nigra	147	0.9	−6.1	9.6	9.1	0.67	0.68	0.13	−0.11	A	1027
Juglans nigra	136	−3.1	−5.5	2.1	2.5	0.80	0.75	−0.20	−0.26	A	950
Ostrya virginiana	131	−4.9	−6.4	15.1	7.1	0.90	0.76	0.29	−0.09	B	1363
Pinus contorta	121	−5.1	−1.6	12.3	9.4	0.95	0.93	−0.21	−0.09	B	943
Pinus monticola	141	−15.7	−9.4	10.6	7.6	0.92	0.91	−0.65	−0.49	A	156
Platanus occidentalis	136	−1.7	−1.8	0	0.5	0.21	0.09	−0.21	−0.09	A	1027
Populus tremuloides	137	−1.9	0.1	0.2	0.2	0.66	0.67	−0.21	−0.01	B	4393
Quercus alba	134	−17.1	−25.7	7.5	8.9	0.65	0.78	0.38	0.07	B	1068
Quercus bicolor	136	−1.9	−6.2	0.1	1.8	0.36	0.52	−0.28	−0.28	A	369
Quercus macrocarpa	139	−5.2	−6.1	−0.2	0	0.66	0.01	−0.66	−0.01	A	1089
Quercus rubra	140	−1.5	−5.4	5.3	8.3	0.71	0.74	−0.46	−0.52	A	1266
Quercus velutina	131	−2.7	−0.4	0.0	0.2	0.38	0.43	−0.38	−0.43	A	942
Salix nigra	54	−14.1	−21.3	0	0	0.87	0.90	−0.68	−0.77	A	1373
Sassafras albidum	63	−13.3	−22.1	0	0.7	0.82	0.93	−0.78	−0.93	A	880
Ulmus americana	132	0.2	−6.1	5.7	6.3	0.65	0.77	−0.11	−0.56	B	2380
Mean		−5.0	−9.2	5.7	5.2	0.67	0.71	−0.21	−0.33		
SE		1.22	1.68	1.53	1.37	0.04	0.06	0.08	0.08		

Mean, average value for all species; SE, standard error.

(2000) using daily mean temperatures and all nine species-specific parameters:

$$D_1 \text{ such as } S_{f,D_1} = \sum_{t_1}^{D_1} R_{f,t} = F_c \quad (1)$$

$$R_{f,t} = \frac{1}{1 + e^{d(T_{a_t} - e)}} \quad (2)$$

$$t_1 \text{ such as } S_{c,t_1} = \sum_{t_0}^{t_1} R_{c,t} = C_c \quad (3)$$

$$R_{c,t} = \frac{1}{1 + e^{[a(T_{a_t} - c)^2 + b(T_{a_t} - c)]}} \quad (4)$$

$$F_c = w\, e^{-zS_{c,t_c}} \quad (5)$$

with t_0 set at 1 September and a, b, c, d, e, w, z, t_c, C_c parameters fitted on phenological observations in natural populations. Parameters a, b, and c define the response function to temperature (also called 'chilling units') that models the effect of 'cold' temperatures in breaking dormancy. Parameters d and e define the response function to temperature (also called 'forcing units') that conditions the effect of 'warm' temperatures during the quiescence or ecodormancy phase, ultimately triggering bud burst. Parameter C_c is the chilling unit threshold at which bud dormancy is broken. Parameters w and z define the inverse exponential function that relates the total amount of chilling units accumulated (i.e. by date t_c) (S_c, t_c) and the amount of forcing units [F_c, Eqn (5)] necessary to reach budburst. For more details, see Chuine (2000).

We fitted these models for each species at each location using daily mean temperatures and leaf unfolding dates from the observations in Ohio, Massachusetts, and Illinois. Parameter estimates were derived by

simulated annealing using the Metropolis algorithm (Metropolis *et al*., 1953). For each species, the best model (i.e. Unified model or a simplified model) was chosen according to its AIC_c (Akaike Information Criterion corrected) (Burnham & Anderson, 2002) fitted on all years available for external validation of the model accuracy. For the 14 species present in the Ohio dataset that had at least 16 years of data, the model parameters were re-fitted with dates from a random 10 years and validated with the remaining years. The limited number of years available from Illinois and Massachusetts did not allow this validation for these populations.

Climate change scenarios and climatic data

For the 20th century simulations, we used the CRU TS 2.0 dataset (Climatic Research Unit, University of East Anglia, Norwich, UK) (New *et al*., 2000), which provides monthly means of daily mean temperature from 1901 to 2000 at $0.5^\circ \times 0.5^\circ$ grid resolution (New *et al*., 2000). Because phenological processes respond strongly to daily weather events (Morin & Chuine, 2005), we generated daily data from the CRU TS 2.0 data using a standard weather generator (e.g. CLIGEN; Nicks *et al*., 1995). Phenological predictions from generated daily temperature data can differ from those using actual temperature records, but the differences are not important in studies of long-term trends at the continental scale (Morin & Chuine, 2005).

For our 21st century simulations, we used daily temperature data from the HadCM3 GCM (Hadley Center for Climate Predictions and Research, UK) (Gordon *et al*., 2000; Pope *et al*., 2000), created under the A2 and B2 IPCC storylines (IPCC, 2001). The A2 and B2 storylines predict a global increase of mean temperature of 3.2 and 1.0 °C, respectively, on average over North America in 2100. As the HadCM3's grid cells were much larger than the CRU grid cells, we disaggregated the HadCM3 data at the $0.5^\circ \times 0.5^\circ$ resolution with an elevation adjustment (Morin & Chuine, 2005).

Given the simulated climatic variables, our models sometimes predict no budburst in a given year for lack of sufficiently cold winter temperatures, which prevents rest completion and thus suppresses breaking dormancy. Experiments assessing changes in leaf unfolding dates under strong levels of warming, using southern populations of some of the species studied, should be carried out to explicitly test the validity of these predictions; we expect that, in reality, these events are likely to be expressed as very late budburst and/or incomplete leaf development (Pop *et al*., 2000).

Simulations

We simulated the annual leaf unfolding date for our 22 tree species over the 20th century with the daily temperature data generated from the CRU TS 2.0 dataset, and over the 21st century for the two storylines A2 and B2 using the HadCM3 daily temperature data. For each species, the model was run on a grid representing North America with a $0.5^\circ \times 0.5^\circ$ resolution (i.e. on 15 888 points), for 1901–2000 and for 2001–2100. Using a daily time step, the model returns a leaf unfolding date for each simulated year. The process was initiated on 1 September of year $n-1$. When parameters corresponding to two or three different populations of the species were available, the model was run separately with each set, and the different simulations averaged using an inverse-squared-distance weighting. For a given point i and year j, the simulated date of leaf unfolding l_{ij} was calculated as

$$l_{ij} = \sum_p \frac{l_{ij}^p}{X_i^p},$$

where $l_{ij}^p$is the model output simulated with the set of parameters fitted from the pth population, and where X_i^p is

$$X_i^p = \frac{d_{ip}^2 / \sum_p d_{ip}^2}{\sum_p \left(d_{ip}^2 / \sum_p d_{ip}^2 \right)}$$

and d_{ip} is the distance between point i and the pth population.

For each grid point i, the simulated dates of leaf unfolding were averaged over each 100-year period (L_i), and the proportion of years with abnormal leaf unfolding (P_i) calculated. As described previously, abnormal leaf unfolding refers to cases in which a model predicts leaves do not unfold because of insufficient chilling to complete rest and break bud dormancy. Changes in L_i and P_i were mapped for each species over its distribution. By averaging values of L_i and P_i over all grid points of a species' distribution, we calculated species-specific mean change in the leaf unfolding date (L_{A2} and L_{B2} for the scenarios A2 and B2, respectively) and the number of years with abnormal leaf unfolding (P) (Table 2).

We also calculated for each species the proportion of occupied area (estimated as a number of grid points) that had a change in leafing date (C):

$$C = \frac{N_h + N_l}{N}$$

with (1) N_h the number of grid points with a leafing date delayed by >3 days, (2) N_l the number of points with a leaf unfolding date advanced by >3 days, and (3) N the total number of grid points within the species'

distribution. Finally, we calculated the species-specific relative change (or direction of change) in leafing date over the distribution (S):

$$S = \frac{N_h - N_l}{N}.$$

Leaf unfolding is advanced by climate change over the entire range when $S < 0$.

Temporal dynamics of the predicted changes in phenology

To compare the simulated changes with those currently observed, we calculated the average rate of change in leaf unfolding date per degree Celsius of warming, for each species and for both scenarios. This rate was obtained by dividing the species-specific mean change in leaf unfolding date L by the average level of warming experienced by each species over its entire range. We also calculated this rate of change per degree Celsius of warming for six 15-year periods, 2001–2015, 2016–2030, 2031–2045, 2046–2060, 2061–2075, 2076–2090, and the 10-year period, 2091–2100. For each grid point i and for each period, we calculated the average date of leaf unfolding and the number of years with abnormal leaf unfolding. For each species and both scenarios, we also calculated the mean leaf unfolding date for the 200 most northerly pixels and the 200 most southerly pixels in the range for each of the 15-year period in the 21st century. We compared the mean leaf unfolding date of each period with the mean leaf unfolding date of the reference period 2001–2015 at the northern and southern periphery of the range.

Interspecific comparisons

For each scenario A2 and B2, we performed correlations of the species-specific indices L, C, S against species-specific leaf unfolding date and two variables characterizing the distribution to detect general patterns in changes across the set of 22 tree species. The two variables characterizing the distribution were the latitude at the northern range limit (in decimal degrees) and the total range area.

Results

Phenological models

The efficiency of the models (percentage of variance explained) by the models (r^2) was >70% in 17 of 23 models (Table 1); the efficiency was >50% in 11 of 14 models tested by external validation. For 15 populations, the best model was not the full Unified model (nine parameters) but a simpler one; the model parameter estimates and the difference in AIC_c values between the best model and the full Unified model are provided in Table 1.

Changes in mean leaf unfolding date

The mean change in leaf unfolding date calculated over all the species is stronger in the B2 than A2 scenario (−5.0 days for A2 and −9.3 days for B2; Table 2). The difference between the two scenarios was significant (paired t-test, $P = 0.03$). The 44 simulations (22 species and 2 scenarios) demonstrate that species will respond to climate change mainly through advance of the leaf unfolding date (39 advances vs. 5 delays), more so in scenario B2 than A2 (Table 2).

Species showed different geographical patterns of a change in their leaf unfolding date (Fig. 1 and Fig. S1). The proportion of a species' distribution area that changed was on average 0.67 in A2 and 0.71 in B2 (C values, Table 2). However, the direction of change varied greatly among species (delay $S > 0$, advance $S < 0$, Table 2, Fig. 1). The proportion of area showing a change (C) for a species was not related to its direction of change (S) for A2 ($r = -0.08$, $P = 0.69$, Pearson's correlation) while it was for B2, ($r = -0.51$, $P < 0.05$, Pearson's correlation).

The responses fall into two groups, some species responding on latitudinal gradients (latitudinal response) and the other to gradients from range center to edge (centrifugal response). Sixteen species showed a greater advance in leaf unfolding date with increasing latitude, i.e. advancement was greater in the northern compared with the southern range, occasionally with a local delay in the south for some species (e.g. *A. saccharum*, *Fraxinus nigra*; Table 2, Fig. 1). Six species showed an overall advance of leaf unfolding date but a different response at the center of the distribution than in the margins (e.g. *Ostrya virginiana*, *Populus tremuloides*; Table 2, Fig. 1).

Focusing on differences between scenarios, we explored the potential involvement of the chilling requirements of species. Species can be classified according to the sensitivity of their phenology to cold temperatures. Some species are 'chilling sensitive', which means that breaking dormancy requires cold temperatures. For these species ($n = 13$), the best model – according to AIC_c values – takes chilling accumulation into account. Others species are 'chilling insensitive' ($n = 6$), and their best phenological model does not require accumulation of chilling units. Three species have both chilling sensitive and chilling insensitive populations (Table 1), an interesting result in its own right; these species with disparate populations are not included in the following comparisons among species. Comparing scenario A2

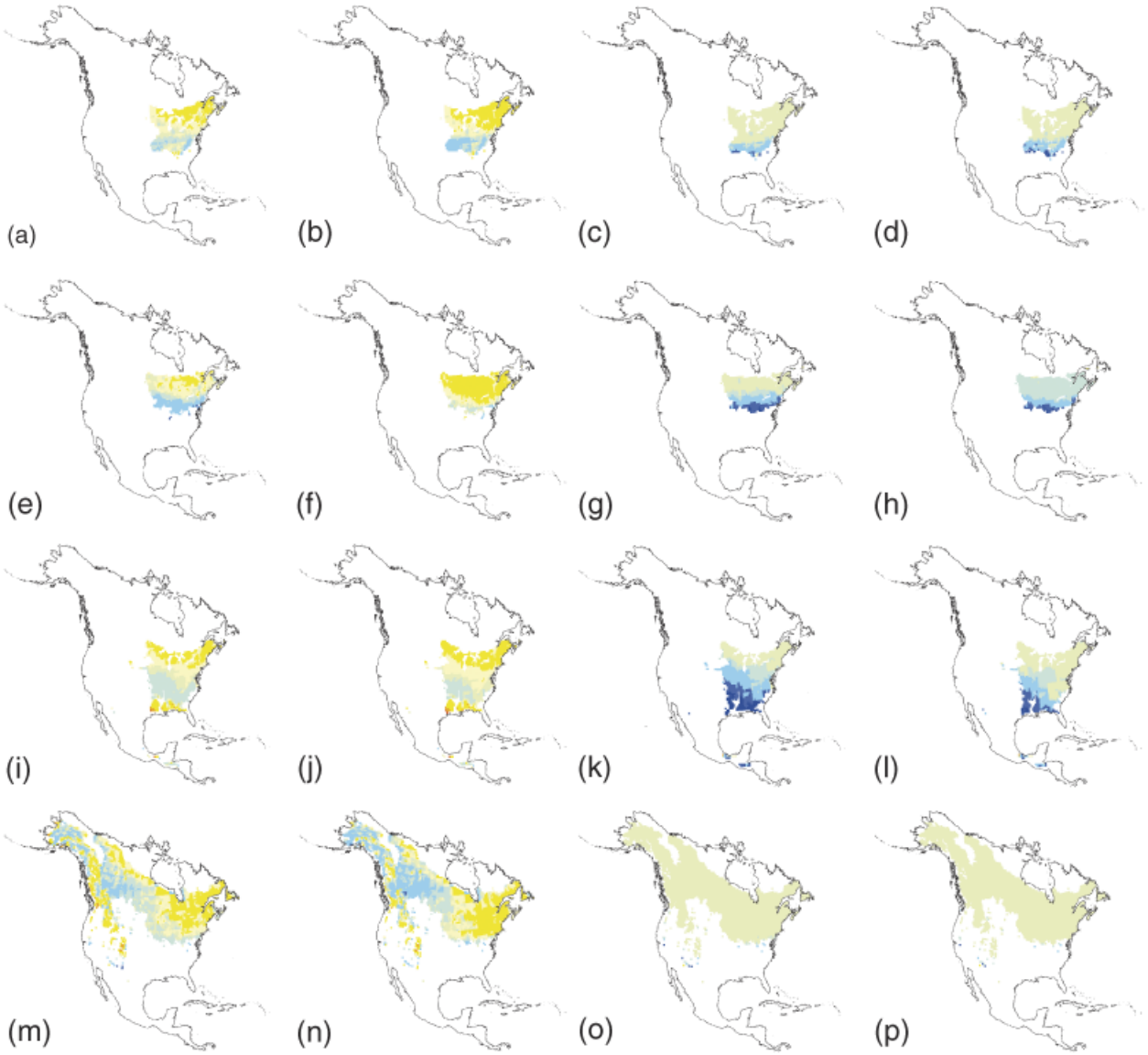

Fig. 1 Mean number of days of change in leaf unfolding date (a, b, e, f, i, j, m, n) and mean change in the number of years when normal leaf unfolding occurs (c, d, g, h, k, l, o, p) between 1901–2000 and 2001–2100 in A2 (left side) and B2 (right side) scenarios for *Acer saccharum* (a–d), *Fraxinus nigra* (e–h), *Ostrya virginiana* (i–l), *Populus tremuloides* (m–p). Left columns: negative values indicate earlier date in 2001–2100 in comparison with 1901–2000. Right columns: negative values indicate less years with leaf unfolding in 2001–2100 in comparison with 1901–2000.

(+3 °C on average over all North America) with scenario B2 (+1 °C), we found that chilling-sensitive species differed significantly in changes of mean leaf unfolding date (−4.3 days for A2 vs. −8.1 days for B2, $P = 0.05$, paired t-test). This difference is smaller and nonsignificant for chilling insensitive species (−6.8 days for A2 vs. −9.8 days for B2, $P > 0.05$, paired t-test).

Furthermore, the date on which dormancy break happens (i.e. when the accumulation of chilling units reaches the fitted threshold – C_{crit} parameter, see 'Materials and methods') occurred later on average under both warming scenarios than under 20th century simulations (Fig. 2), and the delay is larger under A2 than under B2 (−6.8 days for A2 and −2.8 days for B2, averages made on the 13 chilling-sensitive species – using one population per species; Fig. 2).

Abnormal leaf unfolding events

The mean number of years with abnormal leaf unfolding was greater in both warming scenarios than in the 20th century (+5.7 and +5.2 for A2 and B2, respec-

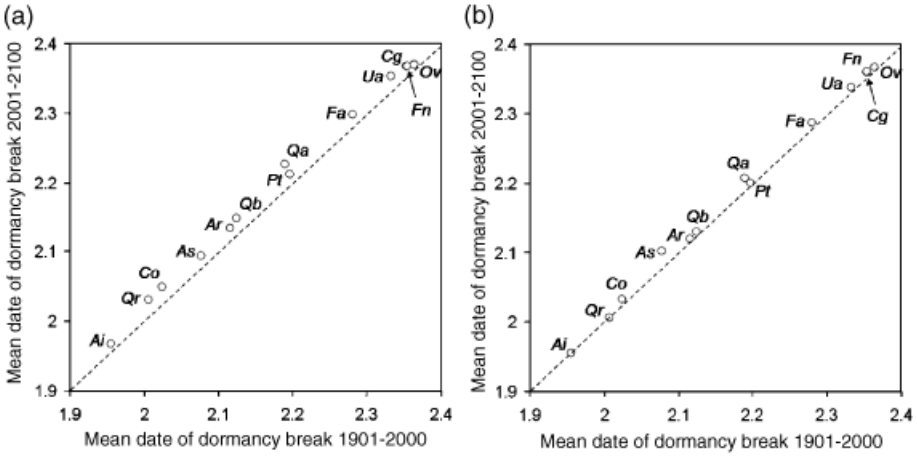

Fig. 2 Mean predicted date of dormancy break for the 13 chilling-sensitive species (one population per species) for the 20th century (*X*-axis) and for the 21st century (*Y*-axis), for scenario A2 (a) and scenario B2 (b). Mean dates were log-transformed. Ai: *Acer saccharinum*; As: *Acer saccharum* (Ohio population); Ar: *Acer rubrum*; Cg: *Carya glabra*; Co: *Carya ovata* (Ohio population); Fa: *Fraxinus americana* (Ohio population); Fn: *Fraxinus nigra*; Os: *Ostrya virginiana*; Pt: *Populus tremuloides* (Ohio population); Qa: *Quercus alba*; Qb: *Quercus bicolor*; Qr: *Quercus rubra*; Ua: *Ulmus americana* (Ohio population).

tively), but the difference between the scenarios was not significant (paired *t*-test $P = 0.42$). Abnormal leaf unfolding affected 14 of 22 species, especially at their southern range edge (e.g. *F. nigra*, Fig. 1). Only *Carya glabra* showed an increase of abnormal leaf unfolding at its northern range edge (Fig. S1). The species showing abnormal leaf unfolding in response to climate change were all chilling-sensitive species (Tables 1 and 2). For these species, the mean change in number of years with abnormal budburst was positively correlated with the mean change in the date on which dormancy break happens, for both scenarios ($r = 0.73$, $P = 0.004$ for A2 and $r = 0.56$, $P = 0.040$ for B2, Pearson's correlations).

Spatiotemporal dynamics of the changes in phenology

In both future scenarios, the mean changes were in general stronger northward. In the north, most species exhibited earlier leaf unfolding from 2015 to 2100 in both scenarios, but the variance among species was larger in A2 than B2 (e.g. Fig. 3a and c). Species responding to the latitudinal gradient had an increasing advance in leaf unfolding date over the 21st century, while species responding on a centrifugal gradient showed more constant change. In the south, advancement tended to be weaker and more species showed a delay at the end of the 21st century in both scenarios. Some species also showed a delay of leaf unfolding after a short period of advance at the beginning of the 21st century (e.g. *F. nigra* and *P. tremuloides* for A2, Fig. 3b). The proportion of years with abnormal leaf unfolding increased throughout the 21st century, especially in the south, and with a stronger intensity in A2 than B2 (results not shown).

Interspecific comparisons

In both future scenarios, the mean change in leaf unfolding date (L_{A2} and L_{B2}) in a species was positively correlated to its mean leaf unfolding date over the 20th century (L), (Table 3, Fig. S2). In other words, early-leafing species tended to show a greater advance in leaf unfolding date, and some late-leafing species actually showed a delay in leaf unfolding.

The proportion of a species' distribution showing a change (C_{A2} and C_{B2}) was negatively related to the mean leaf unfolding date over the 20th century (L) in both scenarios, while the direction of change over all the species' distributions (S_{A2} and S_{B2}) was positively but weakly related to L, although these correlations were only marginally significant (Table 3). This result, however, indicates that early-leafing species may on average experience phenological changes (mainly advancement) over a greater part of their geographical range than late-leafing species. Furthermore, the proportion of change over the whole of the range (C_{A2} and C_{B2}) was negatively related to the mean change in leaf unfolding date for a species in both future scenarios (L_{A2} and L_{B2}), but the correlation was only marginally significant for B2 (Table 3). Basically, the stronger the mean advancement in leaf unfolding date ($L_{A2\,or\,B2} < 0$), the greater is the proportion of the range experiencing a change in this date.

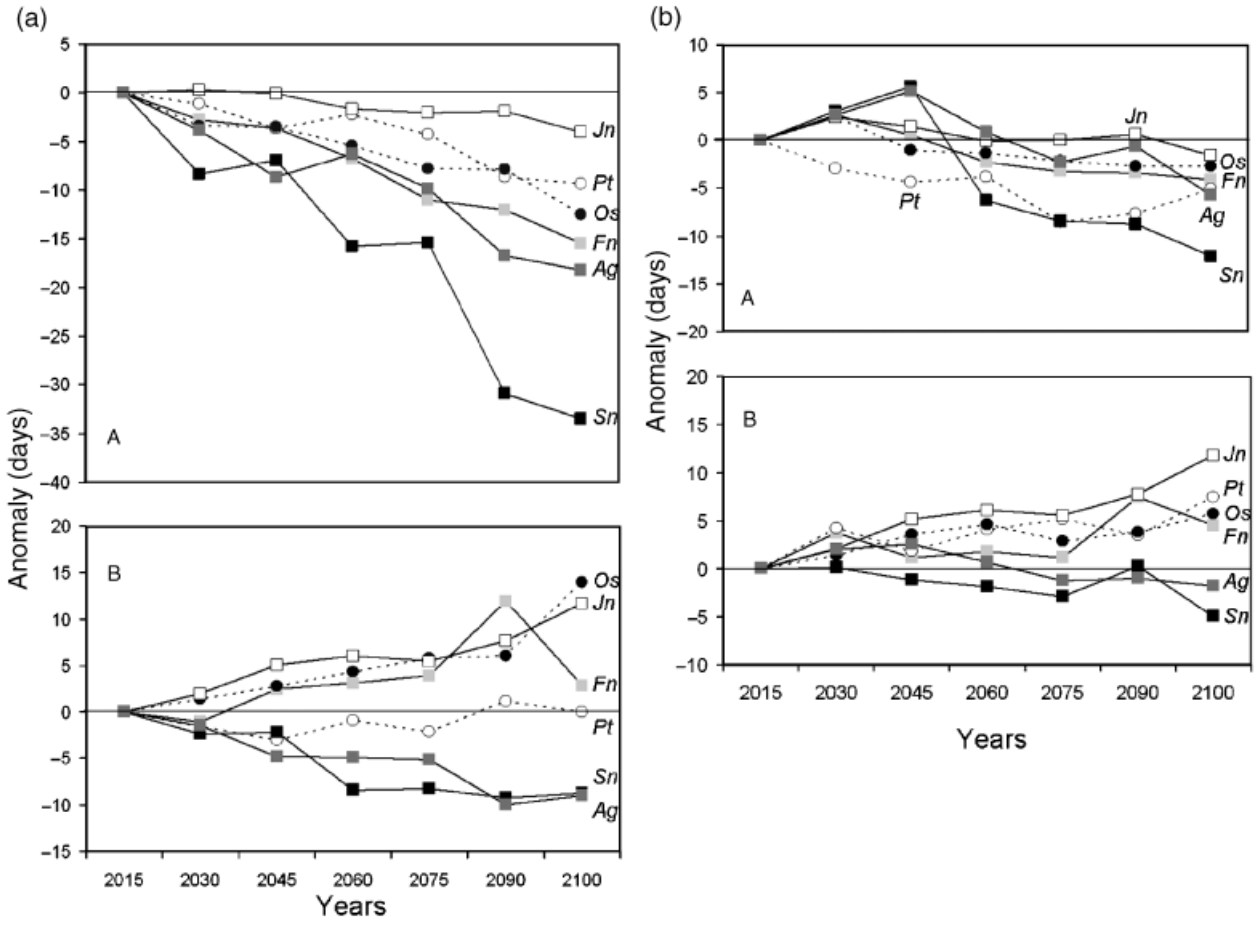

Fig. 3 Mean number of days of change in leaf unfolding date in 2016–2030, 2031–2045, 2046–2060, 2061–2075, 2076–2090, and 2091–2100 relative to 2000–2015, under scenarios A2 and B2 in the north (a and c, respectively) and in the south (b and d, respectively) of distributions (negative numbers indicate earlier dates). For the sake of clarity, only six species are shown, representing (i) the two groups of response (four for A and two for B, see text) and (ii) different chilling sensitivities (three chilling-sensitive species, two chilling nonsensitive species, and one mixed species *Juglans nigra*, i.e. with one chilling-sensitive population and one chilling nonsensitive species, see text). Species of group A: squares (filled: *Salix nigra*; dark gray: *Aesculus glabra*; light gray: *Fraxinus nigra*; open: *J. nigra*); species of group B: circles (filled: *Ostrya virginiana*; open: *Populus tremuloides*). Ag: *Aesculus glabra*; Fn: *Fraxinus nigra*; Os: *Juglans nigra*; Qa: *Ostrya virginiana*; Pt: *Populus tremuloides*; Sn: *Salix nigra*.

The mean change in leaf unfolding date (L_{A2} and L_{B2}) for species was positively related to the total area of distribution (but the correlations were not significant, Table 3). This result may nevertheless suggest that species with larger ranges tend to show stronger changes in their phenology. This relationship may arise because species with larger distribution also have more northerly distributions (Morin & Chuine, 2006) where climate change is predicted to be stronger (IPCC, 2001). Mean change in leaf unfolding date was indeed positively related to the species' northern-range limit, but significantly only for B2 (Table 3). Furthermore, species with more northerly distributions showed a greater variation in leaf unfolding date; the coefficient of variation of leaf unfolding dates of the 14 species in Wauseon and their northern latitude of distribution were positively related ($P<0.05$, $r^2=0.29$, linear regression not shown). This greater range of phenological responses to interannual variation in climate may explain their stronger response to global climate change.

Discussion

Changes in phenology and differences between scenarios

Our results show that on average the date of leaf unfolding of most species in the 21st century will be advanced in response to climate change, extending observed changes in phenology for the second half of the 20th century (Walther *et al.*, 2001; Parmesan & Yohe,

Table 3 Pearson's correlations for both scenarios of (i) species' mean number of days of change in the date of leaf unfolding simulated for the 21st century (L_{A2} and L_{B2}), (ii) total (C_{A2} and C_{B2}), and (iii) relative (S_{A2} and S_{B2}) change in leafing date with species' mean number of days of change in the date of leaf unfolding simulated for the 21st century (L_{A2} and L_{B2}); mean simulated date of leaf unfolding over the 20th century (L); number of pixels ($0.5^\circ \times 0.5^\circ$) occupied by each species' distribution (*Range*); and species' northern latitudinal limit of distribution (*Lat. N*), for 21 species

	L_{A2}		L		Range		Lat. N	
	P-value	*r*	*P*-value	*r*	*P*-value	*r*	*P*-value	*r*
L_{A2}	–	–	0.033	0.45	0.389	0.19	0.655	0.10
C_{A2}	0.028	−0.47	0.084	−0.37	0.852	0.04	0.137	0.33
S_{A2}	0.118	0.34	0.065	0.12	0.591	0.12	0.923	0.02

	L_{B2}		L		Range		Lat. N	
	P-value	*r*	*P*-value	*r*	*P*-value	*r*	*P*-value	*r*
L_{B2}	–	–	0.011	0.53	0.269	0.25	0.043	0.44
C_{B2}	0.091	−0.37	0.059	−0.40	0.871	−0.03	0.748	0.07
S_{B2}	0.161	0.31	0.010	0.19	0.390	0.19	0.202	0.28

For each correlation, *Range* and *Lat. N* have been log-transformed.

2003; Root *et al.*, 2003). Observed rates of change of spring phenology (leaf unfolding and flowering) for temperate trees were -2.9 days decade^{-1} (Chuine, in press) and -3.9 days decade^{-1} (Root *et al.*, 2003) over the last five decades. Previous modeling work using a simpler model and fewer species also predicted results for the end of the 20th century consistent with those currently observed (Richardson *et al.*, 2006). The reported changes in late 20th century tree phenology correspond to a mean advance of 16–24 days per degree Celsius of warming, assuming that the average warming over the last five decades was about 0.6 °C, i.e. $+0.15$ °C decade^{-1} (IPCC, 2001). According to our simulations, changes in leaf unfolding dates would on average be greater in the B2 (with less increase in temperature) than the A2 scenario. The predicted mean advance per degree Celsius in scenario A2 (1.9 day °C^{-1}, on average) is in general less than the currently observed mean advance per degree Celsius (Fig. 4), while, for B2, most species exhibit a mean advance closer to that currently observed (11.8 day °C^{-1}, on average). In the following, we highlight two causes for this result.

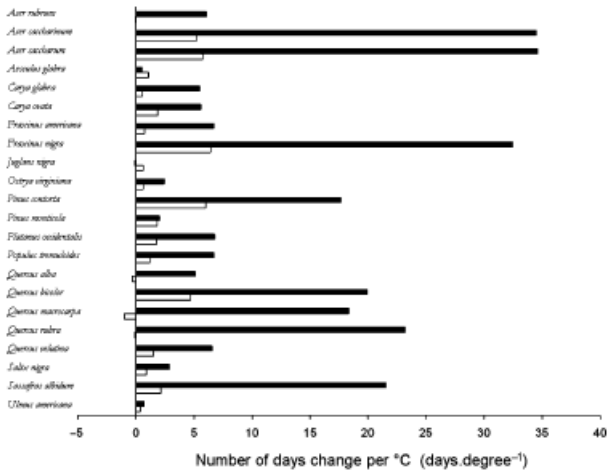

Fig. 4 Mean number of days of change in leaf unfolding date per degree Celsius of warming over 2001–2100 compared with 1901–2000. The level of warming experienced was calculated for each species over its distribution (i.e. by considering only the pixels inside a species' distribution). Positive numbers indicate earlier dates. A2: white bars; B2: black bars. The A2 scenario predicts a global mean increase of 3.2 °C on average over North America, and the B2 scenario a global mean increase of 1.0 °C.

First, these surprising differential responses in species phenology between the two scenarios, as well as the additional prediction of an increase in the occurrence of abnormal leaf unfolding, are due to the dual impact of temperature on phenology. Leaf development is triggered first by low temperatures that break bud dormancy and later by higher temperatures that promote cell expansion and growth. This dual action of temperature is formalized in the models by different response functions defining the course of development in relation to progression of temperature from fall through winter to spring (Kramer, 1995; Chuine, 2000). Thus, warming recorded on an annual basis can in fact act to both lengthen the period of rest and at the

same time accelerate subsequent bud growth. The greater increase in warming under the A2 scenario can lead to delayed or even incomplete fulfillment of the chilling requirement for breaking dormancy that may not be compensated by subsequent acceleration of development. As a result, dormancy break is either delayed (Fig. 2) such that warmer spring temperatures cannot compensate late leaf unfolding, or dormancy break never happens and abnormal leaf unfolding occurs. This hypothesis is strengthened by (i) the comparison of the dates for breaking dormancy (Fig. 2), which show a larger delay under A2 than under B2, and (ii) by the positive relationship between the number of years with abnormal budburst with the change in the date on which dormancy is broken in both scenarios. Consequently, the number of years with abnormal leaf unfolding is higher in the A2 than in the B2 scenario, and, at the end of the 21st century, the mean change in leaf unfolding date is higher in the B2 scenario. In other words, under some climate change scenarios and for some species, a conflict disrupting the evolved phenological control systems can arise in which rising temperatures have a negative effect on breaking dormancy but a positive effect on the rate of bud growth. It is noteworthy that the predicted abnormal leaf unfolding occurs mainly in the southern range of species and that leaf unfolding tends to be less advanced or even delayed to the south but advanced in the north. The most likely explanation is that the effect of warmer temperatures in the southern range, where temperatures are already warmer than in the northern part of the range, is stronger on rest completion than on bud growth during the phase of quiescence that follows breaking of dormancy. These findings are consistent with results from a warming experiment carried out on three European oak species, which showed that leafing phenology was more delayed under the strongest level of warming (Morin *et al*., unpublished).

This possibility of a dual phase influence of warming temperatures on foliar phenology is important because neither observations nor previous predictions of change in phenology have revealed its existence. Murray *et al*. (1989) did suggest that the timing of budburst could be delayed due to climatic change, but this possibility has been discounted because of the numerous studies showing only phenological advancements (e.g. Root *et al*., 2003; Menzel *et al*., 2006). The simulations we have done clearly indicate that Murray's hypothesis should be reconsidered. The classical linear statistical models of foliar phenology cannot predict this trend, but our mechanistic, process-based models suggest this nonlinear, dual-phase dependence in warming responses will begin to be show its effects as global warming increases further (IPCC, 2007).

Second, the contrasting results between A2 and B2 may also be related to different warming dynamics of these two scenarios across the 21st century. Indeed, the fact that chilling insensitive species show an advancement in leaf unfolding date that is slightly greater under the B2 scenario than the A2 scenario cannot be explained as the outcome of a simple delay in dormancy break. This pattern could be explained by differences in the warming dynamic of the two scenarios according to the HadCM3 model simulations. If scenario A2 is on average warmer than B2 at the scale of the 21st century and overall North America, then it appears that B2 implies a stronger warming than A2 in the first part of the 21st century in North America (see Fig. S3). This pattern is even stronger for the temperate latitudes where most of the studied species are distributed. Note that this difference may also contribute to producing the difference in phenological changes between A2 and B2 simulations for other species, but the effect is nevertheless too weak to consistently explain the large difference between the two scenarios across all species.

Differences in changing phenology among species

Phenological changes are highly variable both among species and within their ranges. Species with late unfolding dates advance less on average than those with early unfolding dates, which is consistent with observed phenological changes during the 20th century (Abu-Asab *et al*., 2001). Species with a later phenology may have greater requirements of low temperatures to break dormancy than other species. Under global warming, the requirements for low temperatures are on average fulfilled later, causing a delay in break dormancy. Species with an earlier phenology may have lower chilling requirements so that the warming does not delay breaking dormancy as much as later species, and it accelerates subsequent cell growth, leading, on average, to an advanced leaf unfolding date.

Parmesan & Yohe (2003) reported greater changes in phenology for species with more northern distributions. Although our results corroborate this finding (Table 3), we did not observe a strong pattern, probably because the species we studied have very similar geographic distributions. Nevertheless, our simulations show that the changes in phenology may vary greatly across the geographic range of species. To our knowledge, such differences have never been highlighted at this spatial scale.

Consequences of phenological changes

The earlier leaf unfolding and sometimes abnormal leaf unfolding predicted by our models may have direct

consequences for survival and reproduction through climatic tolerances (Chuine & Beaubien, 2001) as well as indirect effects through biotic interactions (Hughes, 2000; Suttle *et al*., 2007). For instance, phenological changes may induce changes in frost resistance and thus frost damage because of a lower hardiness and an earlier leaf unfolding, as frost events still occur despite warmer average temperatures (Hänninen, 1991; Kramer, 1994; Kellomäki *et al*., 1995; Kramer *et al*., 1996; Leinonen, 1996; Linkosalo *et al*., 2000); the experimental results of Norby *et al*. (2003) are consistent with this possibility. Because the leaf unfolding, flowering, fruit ripening, and senescence phenophases that characterize the annual cycle for a species are usually temporally autocorrelated (Rathcke & Lacey, 1985; Schwartz, 2003) and under strong climatic influence, we can anticipate changes in flowering, fruit maturation, and senescence with implications for failures of adaptation under climate change.

The importance of changing phenology throughout the annual cycle of a species, however, remains to be demonstrated. Although the phenological control systems for a species have been shaped by evolutionary constraints (Lechowicz, 1984), interannual variation in phenological events arises in year-to-year variation in climatic cues governing phenological responses. Process-based phenological models intrinsically take into account this interannual variation, which is necessarily limited as we have illustrated here. The frequency of years with abnormal leaf unfolding may increase with climate change, indicating that the plasticity of phenology will be insufficient to adjust to climate change. Our predictions suggest that some species might experience local extinctions in habitats where their phenology will be strongly affected by the new environmental conditions. This point highlights the relevance of using process-based models to understand which biological mechanisms will be the most sensitive to climate change.

Limits of the predictions

Species regrettably have only one or a few populations with sufficient data to fit leaf unfolding models. To the degree there is ecotypic variation across the range of a species, we therefore must temper our specific predictions, especially for species in which the populations used in calibration were located only toward the northern part of the range (*Acer rubrum*, *C. glabra*, *Quercus alba*, *Quercus rubra*). The phenological responses of southern populations may sometimes be different enough from northern populations to bias some predictions of a model, for example the occurrence of failure to burst bud for lack of sufficient chilling.

It is also the case that the best fitted models did not take the accumulation of chilling units into account for the break of dormancy for eight species (Table 1) because the calibration dataset was unable to detect any chilling requirement for these species (see Hänninen *et al*., 2007). There is, however, no actual experimental evidence that these species are entirely chilling insensitive. The predictions for these species showed on average a stronger response to climate change than the other species, which might be overestimated if these species indeed have chilling requirement which are not taken into account here.

Finally, the calibration of our models does not take long-term acclimation in individual trees or evolutionary shifts in tree populations into account, i.e. the parameter estimates remained fixed during the simulations. For lack of knowledge of genetic controls on critical traits regulating phenological processes, this is simply not yet possible (Wiens & Graham, 2005). We know too little about the genetic determination of control systems for phenological traits and the selective forces that climate exerts on them (Jump & Penuelas, 2005). Our results should be considered baseline predictions of broad trends that do not take account of acclimation and evolution in leafing parameters, but that are likely to be reasonably robust.

Concluding remarks

We have shown that the changes observed in the phenology of tree species during the 20th century will continue during the 21st century, but with significant differences among species and between climate scenarios. Some trends in phenological changes may be reversed by the end of the century because of the bimodality of temperature influence on both chilling and warming cues for phenological control systems. This result is especially important as it can dramatically alter the predictions of process-based models using phenology, especially Dynamic Global Vegetation Models that are coupled with atmosphere–ocean models used to predict climate change. This result highlights the importance and utility of process-based models in studying the impact of climate change on organisms. Statistical phenological models would have led to totally different and possibly erroneous predictions in the tree species we studied. In particular, we show that simple linear extrapolation of phenological trends observed in recent decades cannot be used to predict longer term changes in phenology. Furthermore, our results show that variability in the changes at both inter- and intraspecific levels complicates and perhaps prevents identifying simple, coherent functional groups in the phenological responses to global warming. We have

demonstrated here, however, that broad trends in phenological responses to warming emerge across diverse tree species despite variation in both species-specific controls on phenology and in the geographic distribution of species.

Acknowledgements

The authors are grateful to François Munoz for statistical help, to Paul W. Leadley and Martin T. Sykes for helpful discussions and comments, and to Dennis D. Baldocchi and several anonymous reviewers whose comments greatly improved the manuscript. They also thank Baptiste Hautdidier for mapping help. Support was provided to X. Morin by a Bourse de Docteur Ingénieur du Centre National de la Recherche Scientifique and by a Marie-Curie Outgoing International Fellowship (European Commission's FP6, PHENO-RANGE-EDGE Project, No. 39473). This study was supported by the Institut Français de la Biodiversité and the program Gestion et Impact du Changement Climatique of the French Ministry of Ecology and Sustainable Development.

References

Abu-Asab MS, Peterson PM, Shetler SG, Orli SS (2001) Earlier plant flowering in spring as a response to global warming in the Washington, DC, area. *Biodiversity and Conservation*, **10**, 597–612.

Ahas R, Aasa A, Menzel A, Fedotova VG, Scheifinger H (2002) Changes in European spring phenology. *International Journal of Climatology*, **22**, 1727–1738.

Beaubien EG, Freeland HJ (2000) Spring phenology trends in Alberta, Canada: links to ocean temperature. *International Journal of Biometeorology*, **44**, 53–59.

Boyer WD (1973) Air temperature, heat sums, and pollen shedding phenology of longleaf pine. *Ecology*, **54**, 421–425.

Burnham KP, Anderson DR (2002) Information theory and log-likelihood models: a basis for model selection and inference. In: *Model Selection and Multimodel Inference: A practical Information-Theoretic approach*, (eds Burnham KP, Anderson DR), 2nd edn) pp. 33–74. Springer, Berlin.

Cannell MGR (1985) Analysis of risks of frost damage to forest trees in Britain. In: *Crop Physiology of Forest Trees* (eds Tigerstedt PMA, Puttonen P, Koski V), pp. 153–166. Helsinki University Press, Helsinki.

Cannell MGR, Smith RI (1983) Thermal time, chill days and prediction of budburst in *Picea sitchensis*. *Journal of Applied Ecology*, **20**, 951–963.

Chuine I (2000) A unified model for the budburst of trees. *Journal of Theoretical Biology*, **207**, 337–347.

Chuine I (in press) Forest trees phenology and climate change. In: *Response of Temperate and Mediterranean Forests to Climate Change: Effects on Carbon Cycling, Productivity and Vulnerability* (eds Granier A, Dufrêne E, Pignard G, Loustau D, Dupouey J-L), INRA Editions, Versailles.

Chuine I, Aitken SN, Ying CC (2001) Temperature thresholds of shoot elongation in provenances of *Pinus contorta*. *Canadian Journal of Forest Research*, **31**, 1444–1455.

Chuine I, Beaubien E (2001) Phenology is a major determinant of temperate tree range. *Ecology Letters*, **4**, 500–510.

Chuine I, Cour P (1999) Climatic determinants of budburst seasonality in four temperate-zone tree species. *The New Phytologist*, **143**, 339–349.

Chuine I, Kramer K, Hänninen H (2003) Plant development models. In: *Phenology: An Integrative Environmental Science*, Vol. 39 (ed Schwarz MD), pp. 217–235. Kluwer, the Netherlands.

Chuine I, Rehfeldt GE, Aitken SN (2006) Height growth determinants and adaptation to temperature in pines: a case study of *Pinus contorta* and *Pinus monticola*. *Canadian Journal of Forest Research*, **36**, 1059–1066.

Critchfield WB, Little ELJ (1966) *Geographic Distribution of the Pines of the World. Report No. 991*. U.S. Department of Agriculture, Washington, DC.

Defila C, Clot B (2005) Phytophenological trends in the Swiss Alps, 1951–2002. *Meteorologische Zeitschrift*, **14**, 191–196.

Gordon C, Cooper C, Senior CA *et al*. (2000) The simulation of SST, Sea Ice Extents and Ocean Heat Transports in aversion of the Hadley Centre Coupled Model without flux adjustments. *Climate Dynamics*, **16**, 147–168.

Hänninen H (1991) Does climatic warming increase the risk of frost damage in northern trees? *Plant, Cell and Environment*, **14**, 449–454.

Hänninen H (1996) Effects of climatic warming on northern trees: testing the frost damage hypothesis with meteorological data from provenance transfer experiments. *Scandinavian Journal of Forestry Research*, **11**, 17–25.

Hänninen H, Kramer K (2007) A framework for modelling the annual cycle of trees in boreal and temperate regions. *Silva Fennica*, **41**, 167–205.

Hänninen H, Slaney M, Linder S (2007) Dormancy release of Norway spruce under climatic warming: testing ecophysiological models of bud burst with a whole-tree chamber experiment. *Tree Physiology*, **27**, 291–300.

Hughes L (2000) Biological consequences of global warming: is the signal already apparent. *Trends in Ecology and Evolution*, **15**, 56–61.

Hunter AF, Lechowicz MJ (1992) Foliage quality changes during canopy development of some northern trees. *Oecologia*, **89**, 316–323.

IPCC (2001) *Climate Change 2001: Impacts, Adaptation and Vulnerability. Contribution of the Working Group II to the Third Assessment Report of IPCC*. IPCC, Cambridge.

IPCC (2007) *Climate Change 2007: The Physical Science Basis. Contribution of Working Group I to the Fourth Assessment Report of the Intergovernmental Panel on Climate Change*. Cambridge University Press, Cambridge, UK and New York, NY, USA.

Jump AS, Penuelas J (2005) Running to stand still: adaptation and the response of plants to rapid climate change. *Ecology Letters*, **8**, 1010–1020.

Kellomäki S, Hänninnen H, Kolström M (1995) Computations on frost damage to Scots pine under climatic warming in boreal conditions. *Ecological Applications*, **5**, 42–52.

Kikuzawa K (1991) A cost–benefit analysis of leaf habit and leaf longevity of trees and their geographical pattern. *The American Naturalist*, **138**, 1250–1263.

Kikuzawa K (1995) Leaf phenology as an optimal strategy for carbon gain in plants. *Canadian Journal of Botany*, **73**, 158–163.

Kramer K (1994) A modelling analysis of the effects of climatic warming on the probability of spring frost damage to tree species in the Netherlands and Germany. *Plant, Cell and Environment*, **17**, 367–377.

Kramer K (1995) Phenotypic plasticity of the phenology of seven European tree species in relation to climatic warming. *Plant, Cell and Environment*, **18**, 93–104.

Kramer K, Friend A, Leinonen I (1996) Modelling comparison to evaluate the importance of phenology and spring frost damage for the effects of climate change on growth of mixed temperate-zone deciduous forests. *Climate Research*, **7**, 31–41.

Lechowicz MJ (1984) Why do temperature deciduous trees leaf out at different times? Adaptation and ecology of forest communities. *The American Naturalist*, **124**, 821–842.

Leinonen I (1996) A simulation model for the annual frost hardiness and freeze damage of Scots Pine. *Annals of Botany*, **78**, 687–693.

Linkosalo T (2000) *Analyses of the spring phenology of boreal trees and its response to climate change*. PhD thesis, Department of Forest Ecology, Helsinki.

Linkosalo T, Carter TR, Hakkinen R, Hari P (2000) Predicting spring phenology and frost damage risk of *Betula* spp. under climatic warming: a comparison of two models. *Tree Physiology*, **20**, 1175–1182.

Linkosalo T, Hakkinen R, Hänninen H (2006) Models of the spring phenology of boreal and temperate trees: is there something missing? *Tree Physiology*, **26**, 1165–1172.

Little ELJ (1971) *Atlas of United States Trees, Volume 1, Conifers and Important Hardwoods. Report No. 1146*. U.S. Department of Agriculture, Washington, DC.

Little ELJ (1976) *Atlas of United States Trees, Volume 3, Minor Western Hardwoods. Report No. 1314*. U.S. Department of Agriculture, Washington, DC.

Little ELJ (1977) *Atlas of United States Trees, Volume 4, Minor Eastern Hardwoods. Report No. 1342*. U.S. Department of Agriculture, Washington, DC.

Loustau D, Bosc A, Colin A *et al*. (2005) Modeling climate change effects on the potential production of French plains forests at the sub-regional level. *Tree Physiology*, **25**, 813–823.

Menzel A, Fabian P (1999) Growing season extended in Europe. *Nature*, **397**, 659.

Menzel A, Sparks TH, Estrella N *et al*. (2006) European phenological response to climate change matches the warming pattern. *Global Change Biology*, **12**, 1969–1976.

Metropolis N, Rosenbluth AW, Rosenbluth MN, Teller AH (1953) Equation of state calculations by fast computing machines. *The Journal of Chemical Physics*, **21**, 1087–1093.

Morin X, Chuine I (2005) Sensitivity analysis of the tree distribution model PHENOFIT to climatic input characteristics: implications for climate impact assessment. *Global Change Biology*, **11**, 1493–1503.

Morin X, Chuine I (2006) Niche breadth, competitive strength and range size of tree species: a trade-off based framework to understand species distribution. *Ecology Letters*, **9**, 185–195.

Murray MB, Cannell MGR, Smith RI (1989) Date of budburst of fifteen tree species in Britain following climatic warming. *Journal of Applied Ecology*, **26**, 693–700.

Myneni RB, Keeling CD, Tucker CJ, Asrar G, Nemani RR (1997) Increasing plant growth in the northern high latitudes from 1981 to 1991. *Nature*, **386**, 698–702.

New M, Hulme M, Jones P (2000) Representing twentieth century space–time climate variability. Part II: development of a 1901–1996 monthly grids of terrestrial surface climate. *Journal of Climate*, **13**, 2217–2238.

Nicks AD, Lane LJ, Gander GA (1995) Weather generator. In: *USDA – Water Erosion Prediction Project: Hillslope Profile and Watershed Model Documentation* (eds Flanagan DC, Nearing MA), pp. 2.1–2.22. NSERL, West Lafayette.

Norby RJ, Hartz-Rubin JS, Verbrugge MJ (2003) Phenological responses in maple to experimental atmospheric warming and CO_2 enrichment. *Global Change Biology*, **9**, 1792–1801.

Parmesan C (2006) Ecological and evolutionary responses to recent climate change. *Annual Review of Ecology Evolution and Systematics*, **37**, 637–669.

Parmesan C, Yohe G (2003) A globally coherent fingerprint of climate change impacts across natural systems. *Nature*, **421**, 37–42.

Penuelas J, Boada M (2003) A global change-induced biome shift in the Montseny mountains (NE Spain). *Global Change Biology*, **9**, 131–140.

Pop EW, Oberbauer SF, Starr G (2000) Predicting vegetative bud break in two arctic deciduous shrub species, *Salix pulchra* and *Betula nana*. *Oecologia*, **124**, 176–184.

Pope VD, Gallani ML, Rowntree PR, Stratton RA (2000) The impact of new physical parametrizations in the Hadley Centre climate model – HadAM3. *Climate Dynamics*, **16**, 123–146.

Rathcke B, Lacey EP (1985) Phenological patterns of terrestrial plants. *Annual Review of Ecological Systems*, **16**, 179–214.

Richardson AD, Bailey AS, Denny EG, Martin CW, O'Keefe J (2006) Phenology of a northern hardwood forest canopy. *Global Change Biology*, **12**, 1174–1188.

Root TL, Price JT, Hall KR, Schneider SH, Rosenzweig C, Pounds JA (2003) Fingerprints of global warming on wild animals and plants. *Nature*, **421**, 57–60.

Sarvas R (1972) Investigations on the annual cycle of development on forest trees active period. *Communicationes Instituti Forestalis Fenniae*, **76**, 110.

Sarvas R (1974) Investigations on the annual cycle of development of forest trees. Autumn dormancy and winter dormancy. *Communicationes Instituti Forestalis Fenniae*, **84**, 1–101.

Schwartz MD (1998) Green-wave phenology. *Nature*, **394**, 839–840.

Schwartz MD (2003) *Phenology: An integrative Environmental Science*. Kluwer Academic Publishers, Dordrecht.

Sitch S, Smith B, Prentice IC *et al*. (2003) Evaluation of ecosystem dynamics, plant geography and terrestrial carbon cycling in the LPJ dynamic global vegetation model. *Global Change Biology*, **9**, 161–185.

Smith JW (1915) Phenological dates and meteorological data recorded by Thomas Mikesell at Wauseon, Fulton County, Ohio. *Monthly Weather Review Supplement*, **2**, 21–93.

Spieksma FTH, Emberlin J, Hjelmroos M, Jäger S, Leuschner RM (1995) Atmospheric birch (*Betula*) pollen in Europe: trends and fluctuations in annual quantities and the starting dates of the seasons. *Grana*, **34**, 51–57.

Suttle KB, Thomsen MA, Power ME (2007) Species interactions reverse grassland responses to changing climate. *Science*, **315**, 640–642.

Walther GR, Burga CA, Edwards PJ (2001) *Fingerprints of Climate Change – Adapted Behaviour and Shifting Species Ranges*. Kluwer Academic/Plenum Publishers, New York and London.

Wiens JJ, Graham CH (2005) Niche conservatism: integrating evolution, ecology and conservation biology. *Annual Review of Ecology and Systematics*, **36**, 515–539.

Wolfe DW, Schwartz MD, Lakso AN, Otsuki Y, Pool RM, Shaulis NJ (2005) Climate change and shifts in spring phenology of three horticultural woody perennials in northeastern USA. *International Journal of Biometeorology*, **49**, 303–309.

Supporting Information

Additional Supporting Information may be found in the online version of this article:

Figure S1. Mean number of days of change in leaf unfolding date (a, b, e, f, i, j, m, n, q, r, u, v, y, z, ac, ad, ag, ah, ak, al, ao, ap, as, at, aw, ax, ba, bb, be, bf, bi, bj, bm, bn, bq, br) and mean change in the number of years when leaf unfolding occurs (c, d, g, h, k, l, o, p, s, t, w, x, aa, ab, ae, af, ai, aj, am, an, aq, ar, au, av, ay, az, bc, bd, bg, bh, bk, bl, bo, bp, bs, bt) between 1901–2000 and 2001–2100 in A2 (left side) and B2 (right side) scenarios for *Acer rubrum* (a–d), *Acer saccharinum* (e–h), *Aesculus glabra* (i–l), *Carya glabra* (m–p), *Carya ovata* (q–t), *Fraxinus americana* (u–x), *Juglans nigra* (y–ab), *Pinus contorta* (ac–af), *Pinus monticola* (ag–aj), *Platanus occidentalis* (ak–an), *Quercus alba* (ao, ar), *Quercus bicolor* (as, av), *Quercus macrocarpa* (aw, az), *Quercus rubra* (ba–bd), *Quercus velutina* (be–bh), *Salix nigra* (bi–bl), *Sassafras albidum* (bm–bp), *Ulmus americana* (bq–bt).

Figure S2. The mean change in leaf unfolding date (L_{A2} and L_{B2}) for a species over the 21st century as a function of the mean leaf unfolding date (L) over the 20th century throughout the range of the species ($n = 22$ species; negative numbers indicate earlier dates). Squares: A2 scenario; circles: B2 scenario; full line: regression line for A2 ($r^2 = 0.21$); dashed line: regression line for B2 ($r^2 = 0.28$).

Figure S3. Average difference (over space) of the mean annual temperature simulated by the HadCM3 model according to scenario A2 and scenario B2, for 10-year intervals across the 21st century. Positive values indicate that the predictions for A2 are warmer than the predictions for B2. Filled dots: average over all pixels in North America; open dots: average over all pixels between 55° and 30°N latitude.

Appendix S1. Description of the phenological models simplified from the Unified General Model.

Please note: Wiley–Blackwell are not responsible for the content or functionality of any supporting materials supplied by the authors. Any queries (other than missing material) should be directed to the corresponding author for the article.

